Narrow-bandwidth picosecond pulses by spectral compression of femtosecond pulses in a second-order nonlinear crystal

M. Marangoni,[1*] D. Brida,[1] M. Quintavalle,[2] G. Cirmi,[1] F. M. Pigozzo,[2] C. Manzoni,[1] F. Baronio,[3] A.D. Capobianco,[2] and G. Cerullo[1]

[1]National Laboratory for Ultrafast and Ultraintense Optical Science, INFM-CNR, Dipartimento di Fisica - Politecnico di Milano, Piazza Leonardo da Vinci 32, 20133 Milano, Italy
[2]Dipartimento di Ingegneria dell'Informazione - Università degli Studi di Padova, Via Gradenigo 6/B, 35131 Padova, Italy
[3]Dipartimento di Elettronica per l'Automazione, Università di Brescia, via Branze 38, 25123 Brescia, Italy
[*]Corresponding author: marco.marangoni@polimi.it

Abstract: We introduce a simple approach for the efficient generation of tunable narrow-bandwidth picosecond pulses synchronized to broadband femtosecond ones. Second harmonic generation in the presence of large group velocity mismatch between the interacting pulses transfers a large fraction of the energy of a broadband fundamental frequency pulse into a narrowband second harmonic one. Using a periodically poled stoichiometric lithium tantalate crystal coupled to an infrared optical parametric amplifier, we generated 200-nJ pulses with spectral width lower than 8.5 cm^{-1} and tunability from 720 to 890 nm. Energy scaling and extension of the tuning range are straightforward.

OCIS codes: (190.4410) Nonlinear optics, parametric processes; (190.7110) Ultrafast nonlinear optics; (320.5390) Picosecond phenomena.

References and links

1. P. Guyot-Sionnest, J. H. Hunt, and Y. R. Shen, "Sum-frequency vibrational spectroscopy of a Langmuir film: Study of molecular orientation of a two-dimensional system," Phys. Rev. Lett. **59**, 1597-1600 (1987).
2. L. J. Richter, T. P. Petralli-Mallow, and J. C. Stephenson, "Vibrationally resolved sum-frequency generation with broad-bandwidth infrared pulses," Opt. Lett. **23**, 1594-1596 (1998).
3. D. W. McCamant, P. Kukura, and R. A. Mathies, "Femtosecond broadband stimulated Raman spectroscopy: Apparatus and methods," Rev. Sci. Instrum. **75**, 4971-4980 (2004).
4. P. Kukura, D. W. McCamant, S. Yoon, D. B. Wandschneider, and R. A. Mathies, "Structural observation of the primary isomerization in vision with femtosecond-stimulated Raman," Science **310**, 1006-1009 (2005).
5. G. Cerullo and S. De Silvestri, "Ultrafast optical parametric amplifiers," Rev. Sci. Instrum **74**, 1-18 (2003).
6. A. N. Bordenyuk, H. Jayathilake, and A. V. Benderskii, "Coherent vibrational quantum beats as a probe of Langmuir-Blodgett Monolayers," J. Phys. Chem. B **109**, 15941-15949 (2005).
7. M. Oberthaler and R. A. Höpfel, "Special narrowing of ultrashort laser pulses by self-phase modulation in optical fibers," Appl. Phys. Lett. **63**, 1017-1019 (1993).
8. S. W. Clark, F. Ö. Ilday, and F. W. Wise, "Fiber delivery of femtosecond pulses from a Ti:sapphire laser," Opt. Lett. **26**, 1320-1322 (2001).
9. F. Raoult, A. C. L. Boscheron, D. Husson, C. Sauteret, A. Modena, V. Malka, F. Dorchies, and A. Migus, "Efficient generation of narrow-bandwidth picosecond pulses by frequency doubling of femtosecond chirped pulses," Opt. Lett. **23**, 1117-1119 (1998).
10. S. Laimgruber, H. Schachenmayr, B. Schmidt, W. Zinth, and P. Gilch, "A femtosecond stimulated raman spectrograph for the near ultraviolet," Appl. Phys. B **85**, 557-564 (2006).
11. X. Ribeyre, C. Rouyer, F. Raoult, D. Husson, C. Sauteret, and A. Migus, "All-optical programmable shaping of narrow-band nanosecond pulses with picosecond accuracy by use of adapted chirps and quadratic nonlinearities," Opt. Lett. **26**, 1173-1175 (2001).
12. G. Xu, L. J. Qian, T. Wang, H. Y. Zhu, C. S. Zhu, and D. Y. Fan, "Spectral narrowing and temporal expanding of femtosecond pulses by use of quadratic nonlinear processes," IEEE J. Sel. Top. Quantum Electron. **10**, 174-180 (2004).

#82694 - $15.00 USD Received 2 May 2007; revised 30 May 2007; accepted 31 May 2007; published 3 Jul 2007

13. H. Luo, L. Qian, P. Yuan, and H. Zhu, "Generation of tunable narrowband pulses initiating from a femtosecond optical parametric amplifier," Opt. Express **14**, 10631-10635 (2006).
14. S. Shim and R.A. Mathies, "Generation of narrow-bandwidth picosecond visible pulses from broadband femtosecond pulses for femtosecond stimulated Raman," Appl. Phys. Lett. **89**, 121124 (2006).
15. M. M. Fejer, G. A. Magel, D. H. Jundt, and R. L. Byer, "Quasi-Phase-Matched Second Harmonic Generation: Tuning and Tolerances," IEEE J. Quantum Electron. **28**, 2631-2654 (1992).
16. K. Moutzouris, F. Adler, F. Sotier, D. Träutlein, and A. Leitenstorfer, "Multimilliwatt ultrashort pulses continuously tunable in the visible from a compact fiber source," Opt. Lett. **31**, 1148-1150 (2006).
17. L. Torner, D. Mazilu, and D. Mihalache, "Walking Solitons in quadratic nonlinear media," Phys. Rev. Lett. **77**, 2455-2458 (1996).
18. F. Baronio, C. De Angelis, M. Marangoni, C. Manzoni, R. Ramponi, and G. Cerullo, "Spectral shift of femtosecond pulses in nonlinear quadratic PPSLT Crystals," Opt. Express **14**, 4774-4779 (2006).
19. G. Imeshev, M. A. Arbore, M. M. Fejer, A. Galvanauskas, M. Fermann, and D. Harter, "Ultrashort-pulse second-harmonic generation with longitudinally nonuniform quasi-phase-matching gratings: pulse compression and shaping," J. Opt. Soc. Am. B **17**, 304-318 (2000).
20. U. Sapaev and D. Reid, "General second-harmonic pulse shaping in grating-engineered quasi-phase-matched nonlinear crystals," Opt. Express **13**, 3264-3276 (2005).

1. Introduction

Several time resolved spectroscopy experiments require tunable narrowband picosecond pulses synchronized with broadband femtosecond ones. Examples of such experiments are vibrationally resolved surface sum-frequency generation [1 , 2], which is a powerful probe of molecular order at surfaces and interfaces, and femtosecond stimulated Raman spectroscopy [3, 4], which provides information on the structural evolution of a photoexcited molecule by monitoring the time dependence of its vibrational modes.

Nowadays it is easier to produce widely tunable femtosecond pulses rather than picosecond ones; in fact their much higher peak powers greatly enhance nonlinear optical effects, which can be exploited both for pulse generation, through passive mode-locking, and for wavelength tuning, through optical parametric amplifiers (OPAs) [5]. Several studies have therefore focused on the realization of a "spectral compressor", i.e. a device that can convert with high efficiency a broadband femtosecond pulse into a narrowband picosecond one. Such device is different from a conventional pulse stretcher, which simply increases the pulse duration by introducing a relative delay between the different frequency components of the pulse, while leaving the spectrum unaltered.

Spectral compression is straightforward using linear techniques, which involve spectral filtering of the broadband femtosecond pulses by narrow bandpass filters [6] or slits in the Fourier plane of a zero-dispersion 4*f* pulse shaper [2, 3]; these approaches are however very inefficient, since the loss of energy is approximately proportional to the spectral narrowing. Nonlinear techniques, on the other hand, enable to transfer most of the energy of the broadband pulse into the narrowband one. Self-phase modulation in an optical fiber of a negatively chirped pulse has been shown to lead to bandwidth narrowing [7, 8], but spectral compression limited to a factor of ten has been obtained, and only with low pulse energies. So far, two techniques based on second-order nonlinearities have been proposed for achieving higher energies: sum-frequency generation (SFG) of two oppositely chirped pulses [9, 10] and difference-frequency generation between two pulses with the same chirp [11, 12, 13]. Such techniques are however rather complicated, lossy because of the use of gratings, and only a limited frequency tunability has been obtained. Very recently a picosecond OPA was demonstrated [14], in which the output of a first femtosecond OPA stage is spectrally filtered and used to seed a second narrow-band OPA stage; however, only pulsewidths up to 0.6 ps were obtained, with correspondingly modest compression ratios.

In this paper we propose a simple technique for the spectral compression of femtosecond pulses, based on second-harmonic generation (SHG) in the presence of strong group velocity mismatch (GVM) between the interacting pulses. High GVM implies in fact a very narrow phase-matching bandwidth for the SHG process, and thus the generation of narrowband second harmonic (SH) pulses. In the temporal domain the SH pulse-width is determined by

#82694 - $15.00 USD Received 2 May 2007; revised 30 May 2007; accepted 31 May 2007; published 3 Jul 2007

the difference between the group delays of the fundamental frequency (FF) and SH pulses in the nonlinear crystal. We show that, despite the narrow phase matching bandwidth, the SHG process can have quite high efficiency (up to 40%), thus converting a significant fraction of the broadband FF pulse into a narrowband SH. Wavelength tunability of the SH is achieved by modifying the phase-matching condition in the crystal and accordingly changing the pump wavelength.

Using a 25 mm long periodically-poled stoichiometric lithium tantalate (PPSLT) crystal, we succeeded in generating with 20 % conversion efficiency SH pulses with ~200 nJ energy, spectral width lower than 0.45 nm (8.5 cm^{-1}) and tunability from 720 to 890 nm starting from 40-50 fs near-IR pulses produced by an OPA. By suitable pre-chirping of the FF pulses, we could efficiently reshape the temporal profile of SH pulses, in order to obtain nearly flat-top pulse profiles. Both energy scaling of the pulses and extension of the wavelength tuning range are straightforward.

The paper is organized as follows: Section 2 discusses frequency conversion in the presence of large group velocity mismatch and introduces the main idea behind our method; Section 3 presents the experimental apparatus and results and Section 4 draws some brief conclusions.

2. Frequency conversion in the presence of large group velocity mismatch

In order to get a physical insight into the operation principle of the spectral compressor, let us consider the frequency conversion processes occurring in a second-order nonlinear crystal in the presence of large GVM between FF and SH. Let us assume type I interaction in a crystal of length L and phase-matching for the SHG process: $\omega_{FF} + \omega_{FF} = 2\omega_{FF} = \omega_{SH}$. The bandwidth of the SHG process can be easily determined by letting the FF vary by $\Delta\omega/2$, and thus the SH by $\Delta\omega$. The resulting phase mismatch is, to the first order:

$$\Delta k = \left[\left(\frac{\partial k}{\partial \omega}\right)_{FF} - \left(\frac{\partial k}{\partial \omega}\right)_{SH}\right]\Delta\omega = \left(\frac{1}{v_{gFF}} - \frac{1}{v_{gSH}}\right)\Delta\omega \tag{1}$$

where v_g is the group velocity, so that the SH bandwidth can be written as [15]

$$\Delta\nu_{SH} = 0.886\frac{1}{|\delta|L}, \tag{2}$$

where $\delta = \frac{1}{v_{gFF}} - \frac{1}{v_{gSH}}$ is the GVM between FF and SH. Equation (2) shows that, in the presence of large GVM and long crystals, the SH bandwidth can indeed be quite narrow. As an example, Fig. 1(a) shows the calculated SH bandwidths, as a function of the FF wavelength, for 2.5-cm-long crystals of β-barium borate (BBO) and PPSLT. It can be seen that, for the much more dispersive PPSLT, narrow SH bandwidths around 100 GHz can be generated in a broad spectral range.

Since the phase-matching bandwidth for the SHG process is very narrow in the above-mentioned conditions, one would expect that only a small fraction of the FF spectrum is converted to the SH, leading to poor conversion efficiency. However, with a broadband FF pulse, SH frequencies can be generated also by SFG between the spectral components of the FF pulse that are symmetric with respect to the phase matching frequency ω_{FF}, namely $\omega_1 + \omega_2 = 2\omega_{FF} = \omega_{SH}$, where $\omega_1 = \omega_{FF} + \Delta\omega$ and $\omega_2 = \omega_{FF} - \Delta\omega$. In this case one can write:

$$k(\omega_1) = k(\omega_{FF}) + \left(\frac{\partial k}{\partial \omega}\right)_{FF}\Delta\omega + \frac{1}{2}\left(\frac{\partial^2 k}{\partial \omega^2}\right)_{FF}\Delta\omega^2 + \ldots \tag{3a}$$

$$k(\omega_2) = k(\omega_{FF}) - \left(\frac{\partial k}{\partial \omega}\right)_{FF}\Delta\omega + \frac{1}{2}\left(\frac{\partial^2 k}{\partial \omega^2}\right)_{FF}\Delta\omega^2 + \ldots \tag{3b}$$

the phase mismatch of the SFG process becomes:

#82694 - $15.00 USD Received 2 May 2007; revised 30 May 2007; accepted 31 May 2007; published 3 Jul 2007

$$\Delta k = k(\omega_1) + k(\omega_2) - k(\omega_{SH}) \approx \left(\frac{\partial^2 k}{\partial \omega^2}\right)_{FF} \Delta\omega^2 \tag{4}$$

and the resulting FF bandwidth that can be phase matched is

$$\Delta\nu_{FF} = 0.886 \frac{1}{\left(2\pi L \left|\frac{\partial^2 k}{\partial \omega^2}\right|_{FF}\right)^{1/2}} \tag{5}$$

Equation (5) shows that the SFG process is phase matched to the first order and can therefore very efficiently convert the broadband FF pulse into a narrowband SH one. This effect was first recognized by Moutzouris *et al.* [16]. Figure 1(b) reports the calculated FF phase-matching bandwidths for the SFG process corresponding to the conditions of Fig. 1(a); it can be seen that, even for the more dispersive PPSLT, relatively broad bandwidths ranging from 5 to 10 THz can be converted.

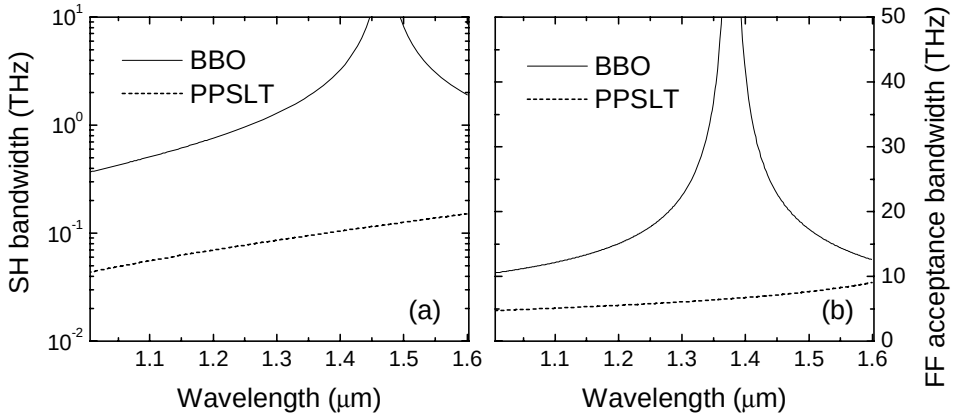

Fig. 1. (a). calculated SH bandwidths, as a function of the FF wavelength, for 2.5-cm-long BBO and PPSLT crystals; (b) calculated FF phase-matching bandwidths for the SFG process in the same crystals.

The use of periodically poled crystals for the spectral compressor, besides the large GVM values, has two additional advantages: (i) due to the large second-order nonlinear coefficients, SHG takes place at relatively low intensities, well below the onset of parasitic third-order processes which spoil the spatial and spectral characteristics of the pulses; (ii) the nonlinear interaction is free from spatial walk-off, which is particularly important to optimize the spatial overlap between FF and SH over long distances.

While allowing some physical insight, the above-described approach provides only a crude description of the frequency conversion process. In order to investigate the temporal properties of the SH pulses, and to identify the conditions for the generation of narrowband SH pulses with high efficiency and optimized temporal profiles, it is necessary to perform a more accurate numerical simulation of the frequency conversion process in the presence of large GVM. By assuming plane waves propagating in z direction and a time frame moving with the linear group velocity of the FF pulse, the governing equations are [17]:

$$j\frac{\partial \mathrm{w}}{\partial z} - \frac{k''_{FF}}{2}\frac{\partial^2 \mathrm{w}}{\partial t^2} + \frac{\chi^{(2)}\pi}{\lambda_{FF} n_{FF}}\ \mathrm{vw}^* e^{-j\Delta kz} = 0 \tag{6a}$$

#82694 - $15.00 USD Received 2 May 2007; revised 30 May 2007; accepted 31 May 2007; published 3 Jul 2007

$$j\frac{\partial \mathrm{v}}{\partial z} - j\delta\frac{\partial \mathrm{v}}{\partial t} - \frac{k''_{SH}}{2}\frac{\partial^2 \mathrm{v}}{\partial t^2} + \frac{\chi^{(2)}\pi}{\lambda_{FF} n_{SH}}\mathrm{w}^2 e^{j\Delta kz} = 0 \tag{6b}$$

where $w(z,t)$ and $v(z,t)$ are the electric field envelopes (in V/m) of the FF and SH waves, respectively, $k''=\frac{\partial^2 k}{\partial \omega^2}$ is the group velocity dispersion, n is the refractive index, λ the wavelength; $\Delta k = 2k_{FF} - k_{SH} + 2\pi/\Lambda$ is the effective mismatch, where Λ is the poling period of the crystal, and $\chi^{(2)}$ is the effective nonlinear coefficient ($\chi^{(2)}=4/\pi d_{33}$ for PPSLT). Equations (6) are numerically integrated by a split-step beam-propagation method in which the nonlinear propagation step is solved by a fourth order Runge-Kutta algorithm in the time domain, while the dispersive linear propagation step is solved by Fourier transformation in the frequency domain. The following initial conditions, corresponding to the experimental ones, are used: input gaussian pulses with spectral bandwidth 10.7 THz, corresponding to a transform-limited (TL) FF pulse-width τ_{FF} = 40 fs, central wavelength λ_{FF} = 1420 nm, crystal length L = 25 mm, corresponding to 2.5 times the FF dispersive length ($L_D=\tau_{FF}^2/2|k''|$), and to 250 times the GVM length ($L_{GVM}=|\delta|\tau_{FF}$) in PPSLT.

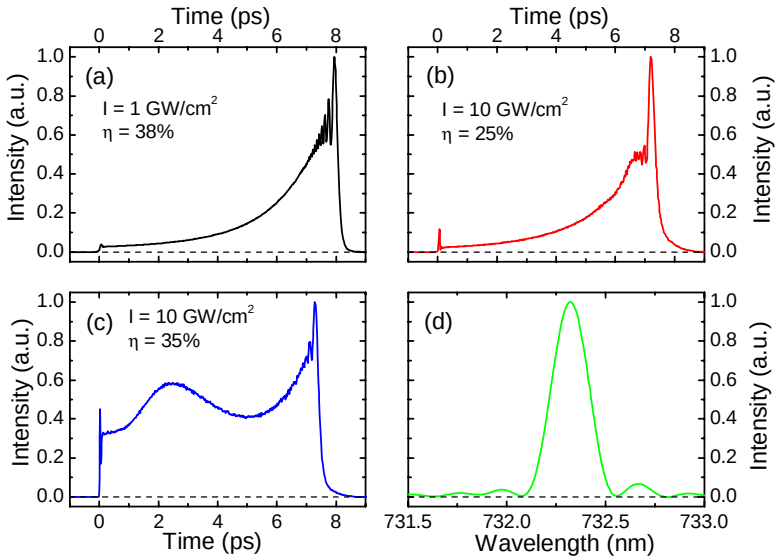

Fig. 2. (a). Calculated SH pulse profile for TL FF pulses with Δk = 0 and peak intensity 1 GW/cm^2; (b) same as (a) for Δk = -25000 m^{-1} and peak intensity 10 GW/cm^2; (c) same as (b) for input pulse with a –2640 fs^2 negative chirp; (d) SH spectrum corresponding to case (c).

Figure 2(a) shows the numerically simulated SH intensity profile for a phase-matched interaction (Δk = 0), a transform-limited (TL) input pulse and a FF peak intensity of 1 GW/cm^2. The SHG efficiency is remarkably high (38%) despite the rather low input intensity, and the SH spectrum is as expected very narrow (120 GHz FWHM, corresponding to 4 cm^{-1}) and reduced by two orders of magnitude with respect to the FF one. In these conditions however two main drawbacks can be identified: i) a modest SH output energy, due to the fact that crystals as thin as periodically-poled ones do not allow scaling the energy with the beam spot size for a given optimum intensity, ii) an highly asymmetric SH pulse profile, consisting of a strong peak generated in the first part of the crystal followed by a long weak tail generated in the second part. The first drawback can be overcome by working with suitably phase mismatched conditions, so as to decrease the strength of the nonlinearity. Figure 2(b) reports the results for Δk = - 25000 m^{-1}, allowing an higher FF peak intensity of 10 GW/cm^2 (and thus an higher SH energy) for a comparable conversion efficiency. Note that it is

#82694 - $15.00 USD Received 2 May 2007; revised 30 May 2007; accepted 31 May 2007; published 3 Jul 2007

preferable to choose negative Δk values due to the fact that they do not lead to the onset of self-focusing nonlinearities induced by cascaded SHG [18], and they also avoid FF pulse break-up. The asymmetric SH pulse profile is due to the combined effect of pump depletion, occurring during the first few GVM lengths, and linear dispersion, both concurring to reduce the FF peak intensity during propagation and thus the SHG efficiency. These effects can be countered by introducing a negative chirp on the FF pulse. Figure 2(c) shows the results for a pump pulse with identical energy and spectrum as in Fig. 2(b) but with a - 2640 fs^2 chirp, opposite to that introduced by the PPSLT crystal. In this case the peak intensity at the crystal input is reduced by a factor of ~3, i.e. roughly the ratio between the crystal length and the dispersion length, and a nearly flat-top SH pulse profile is obtained, since pump depletion is compensated by linear pulse compression of the pump pulse itself; the conversion efficiency in this case is enhanced to 35%. The presence of this chirp does not affect the SH spectrum (120 GHz bandwidth), displayed in Fig. 2(d). Numerical simulations thus validate the operation of the spectral compressor, demonstrating that spectral narrowing by over two orders of magnitude with efficiency higher than 30 % can be obtained, and that chirping of the pump pulses allows for nearly symmetric SH temporal profiles.

3. Experimental results

To demonstrate our technique we chose to use a PPSLT crystal due to its strong nonlinearity and high optical damage threshold. The crystal has 25 mm length, 0.5 mm thickness and is provided with several poling periods allowing the phase-matching condition, and thus the SH wavelength, to be easily changed. The FF pulses are generated by a near-IR OPA pumped by 800-nm, 50-fs, 50-μJ pulses from an amplified Ti:sapphire laser at 1 kHz. The OPA is seeded by the white-light continuum generated in a 3-mm-thick sapphire plate and employs a single pass in a 3-mm-thick BBO crystal cut for type II phase matching (θ=28°); it produces nearly

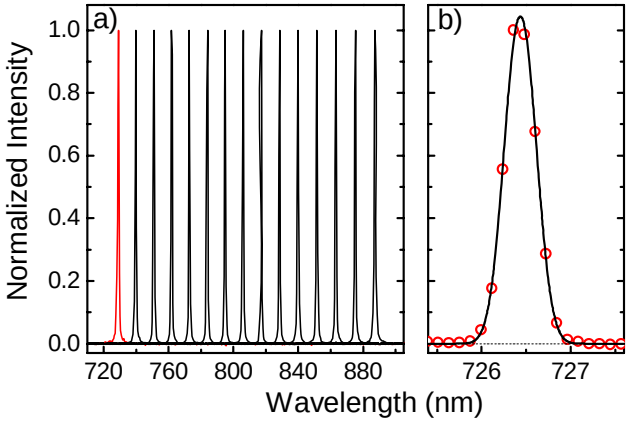

Fig. 3 (a). Sequence of SH spectra for different poling periods of the PPSLT crystal. (b) zoom of a spectrum for Λ = 17.7 μm; points correspond to experimental values and solid line to a gaussian fit.

transform-limited pulses, tunable from 1.2 to 1.8 μm, with 40-50 fs duration and energy up to 4 μJ. The OPA pulses are sent to a dispersive delay line consisting of a pair of Brewster-cut SF10 prisms at a 40-cm distance and, after suitable attenuation, are focused on the crystal input face with a spot size of 180 μm. The prism pair introduces, around 1.4 μm wavelength, a second order dispersion of –3100 fs^2, nearly opposite to that caused by the PPSLT crystal (2640 fs^2) and the refractive optics. Under such conditions the FF pulses exiting the crystal are in fact nearly TL, as verified by measuring their autocorrelation. The SH spectrum is recorded with a spectrometer (Oriel Instaspec IV) equipped with a 1200 lines/mm grating and a 50 μm

#82694 - $15.00 USD Received 2 May 2007; revised 30 May 2007; accepted 31 May 2007; published 3 Jul 2007

entrance slit, allowing for a 0.4 nm spectral resolution. The temporal profile of the SH pulses is characterized both by non-collinear autocorrelation in a 1-mm-long BBO crystal and by cross-correlation with a fraction of the 800-nm Ti:sapphire pulses. The cross-correlation trace closely follows the SH intensity profile since its duration is nearly 2 order of magnitude higher than that of the 800-nm gate pulses.

Figure 3(a) shows a sequence of SH spectra obtained by changing the poling period from Λ = 17.7 μm (722 nm) to Λ = 26.3 μm (887 nm). Such a large tuning range of course requires changing correspondingly the FF produced by the OPA. For a given poling period, fine wavelength tuning is achieved by varying the crystal temperature. As an example, for Λ = 17.7 μm the SH wavelength could be tuned from 722 nm to 736 nm by increasing the temperature from 25 °C to 200 °C. Figure 3(b) is a zoom image of the SH spectrum at 726 nm, exhibiting a FWHM width of 0.45 nm, which is quite close to the ≈0.2 nm (110 GHz) expected value after deconvolving the instrumental response. This corresponds to a rather high spectral compression ratio of ~ 100. It is worth noting that the SH spectra are substantially independent on phase-mismatch between FF and SH waves, input pulse energies and pump pulse chirp. They only differ in terms of spectral width, with the narrowest spectra (0.45 nm) corresponding to the shortest wavelengths and the broadest spectra (0.6 nm) to the longest wavelengths, for which GVM between FF and SH waves is lower.

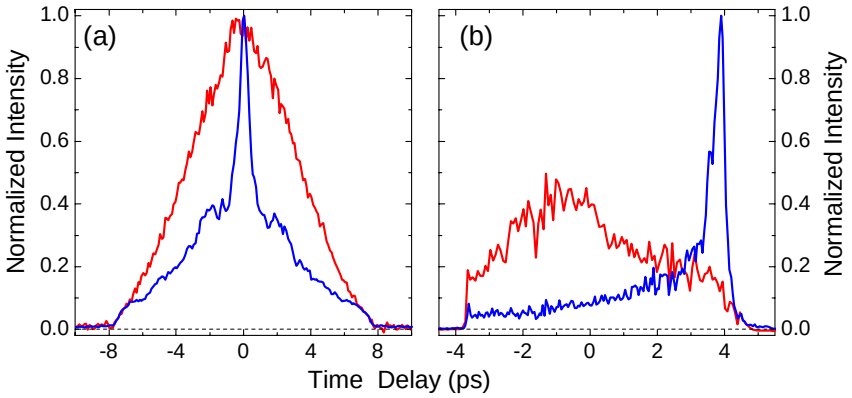

Fig. 4. (a). autocorrelations and (b) cross-correlations of the SH pulses exiting the Λ = 17.9 μm PPSLT crystal for TL (blue lines) and negatively chirped (red lines) input pulses.

Figure 4 shows the temporal characteristics of the SH pulses at 722 nm for a FF input pulse energy of 1 μJ and a Δk = -19000 m^{-1}. This energy corresponds to an input peak intensity of 25 GW/cm^2 in the case of TL pump pulses (blue curves) and of 7.5 GW/cm^2 when chirped pump pulses are used (red curves). The chirp does not affect significantly the SHG efficiency, in both cases close to 20 %, but it strongly modifies the SH temporal profile. For a TL pulse, both auto- and cross-correlation show a highly asymmetric pulse shape, consisting of a sharp initial spike followed by a long tail, in agreement with the numerical simulations reported in Figs. 2(a)-2(b). This effect is removed for a negatively chirped pulse, which produces a more regular pulse profile, confirming the results of Fig. 2(c).

4. Conclusions

In conclusion, we have demonstrated a simple approach for the generation of tunable picosecond pulses synchronized with femtosecond ones. This method exploits the second harmonic generation process in the presence of large GVM to efficiently transfer the energy of a broadband FF pulse into a narrowband SH one: coupled to an OPA, it allows the generation of broadly tunable picosecond pulses. By SHG of an infrared OPA in a 25-mm-long PPSLT crystal, we obtained pulses tunable from 720 to 890 nm with ≈100 GHz bandwidth and energy

#82694 - $15.00 USD Received 2 May 2007; revised 30 May 2007; accepted 31 May 2007; published 3 Jul 2007

up to 200 nJ. The output energy is limited by the small thickness of the PPSLT crystal (0.5 mm aperture), which requires tight focusing and thus leads to the optimum intensities with relatively low input energy. It is straightforward to increase the energy by at least one order of magnitude using thicker crystals (2 mm aperture periodically poled crystals are commercially available). Extension of the tuning range in the visible and UV wavelength ranges is also possible, by choosing suitable nonlinear crystals and OPA systems. We have shown that the temporal profile of the narrowband SH pulse can be simply controlled by introducing a suitable negative chirp on the FF pulse. A more sophisticated temporal shaping could be implemented by tailoring the nonlinear optical coefficient along the propagation direction using a suitably designed aperiodic poling [19, 20].

Acknowledgments

We acknowledge financial support from the project PRIN 2005 “Spectral and temporal control of femtosecond pulses by second order nonlinear processes.”

#82694 - $15.00 USD Received 2 May 2007; revised 30 May 2007; accepted 31 May 2007; published 3 Jul 2007